

Research Article

Second Law Analysis of Al_2O_3 -Water Nanofluid Turbulent Forced Convection in a Circular Cross Section Tube with Constant Wall Temperature

Vincenzo Bianco,¹ Oronzio Manca,² and Sergio Nardini²

¹ University of Genoa, DIME/TEC, Division of Thermal Energy and Environmental Conditioning, Via All'Opera Pia 15/A, 16145 Genova, Italy

² Seconda Università degli Studi di Napoli, Dipartimento di Ingegneria Industriale e dell'Informazione, Via Roma 29, 81031 Aversa, Italy

Correspondence should be addressed to Vincenzo Bianco; vbianco@libero.it

Received 27 June 2013; Accepted 11 September 2013

Academic Editor: Liqiu Wang

Copyright © 2013 Vincenzo Bianco et al. This is an open access article distributed under the Creative Commons Attribution License, which permits unrestricted use, distribution, and reproduction in any medium, provided the original work is properly cited.

The present paper proposes an analysis based on the second principle of thermodynamics applied to a water- Al_2O_3 nanofluid. The nanofluid flows inside a circular section tube subjected to constant wall temperature. The aim of the investigation is to understand, by means of an analytical model, how entropy generation within the tube varies if inlet conditions, particles concentration, and dimensions are changed. To gather these information is of fundamental importance, in order to optimize the nanofluid flow. The results show that according to the inlet condition, there is a substantial variation of the entropy generation, particularly when Reynolds number is kept constant there is an increase of entropy generation, whereas when mass flow rate or velocity are taken constant, entropy generation decreases.

1. Introduction

The study of nanofluids has attracted the interest of many researchers all around the world, because of the unique heat transfer capabilities shown by such a new category of fluids. A nanofluid is a suspension of nanoparticles, usually metal oxides, within a base fluid, such as water, glycol, or mineral oil. Suspending nanoparticles in a fluid leads to an increase of its thermal properties; in particular, nanoparticles contribute to increase thermal conductivity, resulting in a mixture with higher conductivity with respect to the base fluid.

On the contrary, the viscosity of the mixture increases, determining higher pressure losses. Therefore, there is a competing behavior of thermal conductivity and viscosity which both increase with particles concentration, thus it is necessary to establish an optimal value.

Researchers are engaged in developing different kinds of studies regarding nanofluids in order to describe

thermophysical properties, natural and forced convection flow, and the application in different devices.

Recently, Khanafer and Vafai [1] presented a critical synthesis of the variants within the thermophysical properties of nanofluids. Correlations for effective thermal conductivity and viscosity are synthesized and developed in this study in terms of pertinent physical parameters based on experimental data available in the literature. Also, Corcione [2, 3] proposed different models to estimate thermal conductivity and dynamic viscosity of nanofluids developed by making a synthesis of experimental data available in the literature.

Fan and Wang [4], instead, proposed a review on the thermal conductivity studies about nanofluids, and they focused on the physical mechanisms which cause the enhancement of nanofluids conductivity. Buongiorno [5] investigated the mechanisms which cause the enhancement of the heat exchange in nanofluids. He analyzed all the possible physical phenomena that can influence heat transfer in nanofluids,

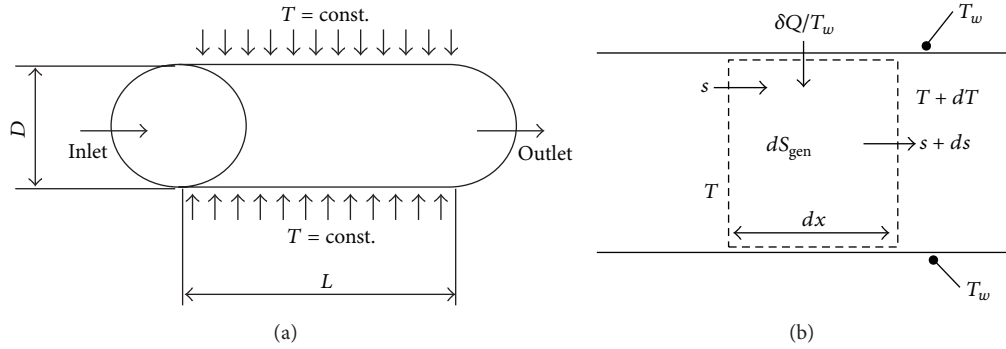


FIGURE 1: (a) Schematic of the configuration under investigation. (b) Control volume for the entropy balance.

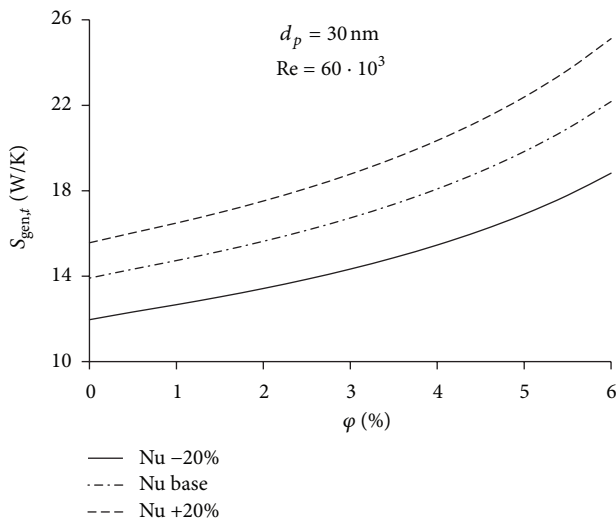


FIGURE 2: Effect of experimental deviations of Nu (16) on the thermal entropy generation.

and he proposed a correlation to estimate Nusselt number for nanofluid turbulent convection in a tube.

Other researchers performed different numerical analysis on the convection of nanofluids, in order to understand the possibility to use nanofluids in practical applications and to assess which are the best methodologies to simulate nanofluid flow.

Khanafar et al. [6] were the first to propose a numerical model to study natural convection in an enclosure filled with a Cu-water nanofluid. They presented a correlation of the average Nusselt number for various Grashof numbers and volume fractions.

Bianco et al. [7] and He et al. [8] proposed for the first time the application of the discrete phase model to the simulation of nanofluids convection. They performed a full two-phase simulation, modeling the nanoparticles with a Lagrangian approach and the base fluid by means of the usual Eulerian methodology. Subsequently, Tahir and Mital [9] successfully utilized this approach to simulate the developing laminar forced convection flow of alumina-water

nanofluid in a circular tube subjected to a uniform wall heat flux. They analyzed the effects of particle diameter, Reynolds number, and volume fraction of the particles on the average heat transfer coefficient. Instead, Behzadmehr et al. [10, 11] were the first to simulate nanofluid convection flow by means of the mixture model, demonstrating the accuracy of this methodology, which cannot explicitly account for two separate phases, but it allows considering the particles with an additional term in the momentum equation and by adding a concentration equation. The validity of this approach was also confirmed by Bianco et al. [12, 13].

Hejazian and Moraveji [14] developed a comparison between single-phase model and mixture model, highlighting the limited deviation of the mixture model with respect to experimental results. Moraveji and Esmaili [15] tested both single-phase and two-phases CFD modeling of laminar forced convection flow of nanofluids in a circular tube under constant heat flux. They detected a good agreement between the numerical results and experimental data.

Other researchers focused their interest on the application of nanofluids in various kinds of devices, in order to understand if better performances might be achieved by employing nanofluids.

Wong and de Leon [16] sustain that nanofluids can be utilized where straight heat transfer enhancement is paramount as in many industrial applications, nuclear reactors, transportation, and electronics, as well as biomedicine and food processing.

Shafahi et al. [17–19] proposed the application of nanofluids in different kinds of heat pipe. They demonstrated the existence of an optimal concentration which maximizes heat transfer capillary limits. Manca et al. [20] applied nanofluids to ribbed channels in order to increase the heat transfer capabilities of such devices. They performed a numerical investigation showing a heat transfer enhancement and corresponding increase of required pumping power. Krishna Sabareesh et al. [21] investigated the effect of dispersing a low concentration of TiO_2 nanoparticles in the mineral oil based lubricant, on its viscosity and lubrication characteristics, as well as on the overall performance of a vapor compression refrigeration system using R12 (Dichlorodifluoromethane) as the working fluid. They detected enhancement in the COP

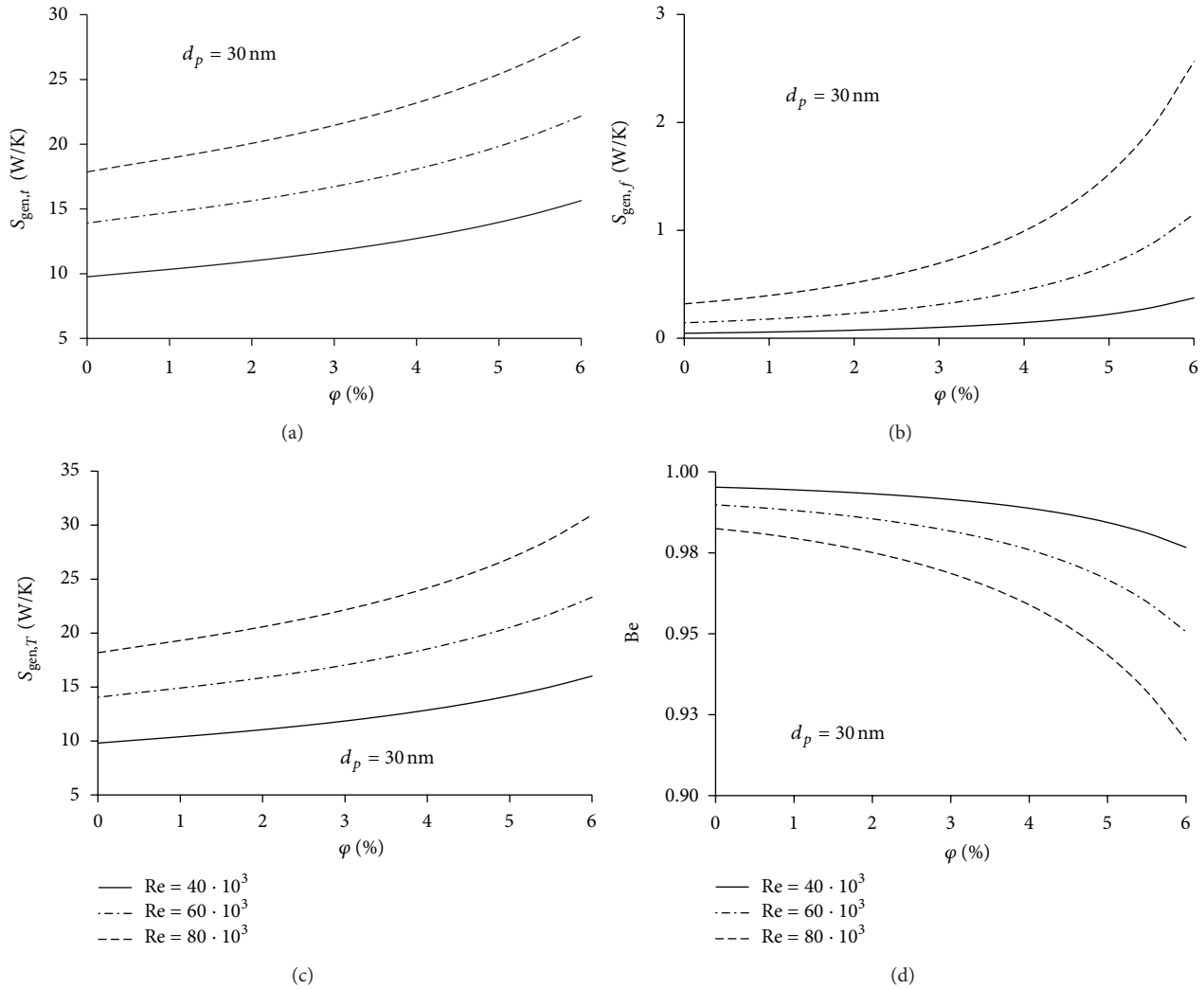


FIGURE 3: Entropy generation for constant Re number inlet condition and for $d_p = 30$ nm: (a) thermal entropy generation; (b) frictional entropy generation; (c) total entropy generation; (d) Bejan number.

of the refrigeration system and the existence of an optimum volume fraction at low concentrations of nanoparticles suspended in the mineral oil.

Mahian et al. [22] proposed a review about the applications of nanofluids in the field of solar thermal engineering systems. They found that most of the work consider the effects of nanofluids on the performance of solar collectors and solar water heaters from the efficiency, economic, and environmental considerations viewpoints. In addition, they highlight some works on the applications of nanofluids in thermal energy storage, solar cells, and solar stills.

All the mentioned literature focus on the study of the fundamental heat transfer phenomena or applications involving nanofluids, and it is based on the first law of thermodynamics, which is not sufficient to add consideration about the energy efficiency of these kinds of systems. It is therefore necessary to enlarge the focus and to base the analysis also on the second law of thermodynamics.

According to this, different authors start to propose investigations taking into account entropy generation in nanofluid flow.

Mahian et al. [23, 24] analyzed entropy generation between two corotating cylinders using nanofluids. They found that the TiO_2 -water nanofluid represent the optimal choice for this kind of configuration.

Leong et al. [25, 26] studied the entropy generation of turbulent convection of nanofluids subjected to constant wall temperature and analyzed entropy generation of three different types of heat exchangers working with nanofluids. They determined the optimal working conditions for the investigated devices. Moghaddami et al. [27] and Singh et al. [28] proposed two interesting theoretical investigations of entropy generation of nanofluids convection. They showed the existence of different optimal working points according to the flow features, but they do not consider the influence of particles diameter.

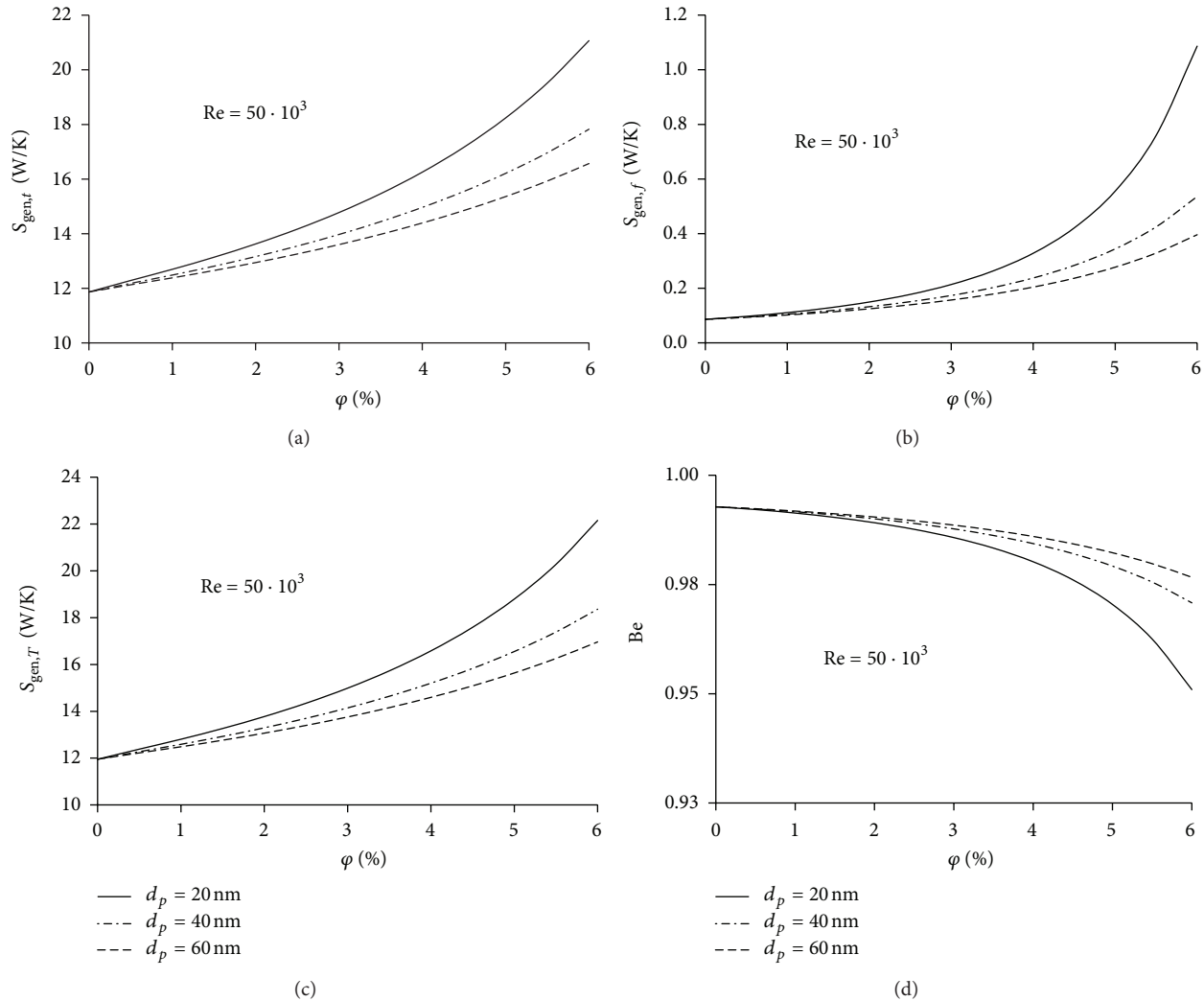


FIGURE 4: Entropy generation for constant Re number inlet condition ($Re = 50 \cdot 10^3$) and different particles dimensions: (a) thermal entropy generation; (b) frictional entropy generation; (c) total entropy generation; (d) Bejan number.

Developing turbulent-forced convection flow of a water- Al_2O_3 nanofluid in a square tube, subjected to constant and uniform wall heat flux, was numerically investigated by Bianco et al. [29]. A simple analytical procedure was proposed to evaluate the entropy generation, and its results were compared with the numerical calculations, showing a very good agreement. An entropy generation analysis was also proposed in order to find the optimal working condition for the given geometry under given boundary conditions. Very recently, Bianco et al. [30] proposed an analytical investigation to analyze entropy generation in a tube subjected to constant wall heat flux. The influence of particles concentration and dimensions as well as the influence of inlet conditions were assessed.

The present paper has the aim to develop an analytical investigation of entropy generation of Al_2O_3 -water based nanofluid in turbulent convection inside a circular cross section tube, subjected to constant wall temperature, in order to understand if there are optimal working conditions.

Different inlet conditions, namely, constant Re, constant mass flow rate and constant velocity, concentrations, and dimensions, are considered in order to assess their influence on the entropy generation.

It is important to highlight that, to the best of the authors' knowledge, the effect of particles dimensions on the entropy generation of a tube subjected to constant wall temperature is analyzed for the first time in this paper.

The information and comments contained in the present work are believed to be useful to pursue the optimal design of thermal devices; in particular, the system considered in the present paper is a very common configuration, utilized in numerous kind of applications.

2. Methodology

2.1. Description of the Problem. The problem considered in the present paper consists of the analysis of average entropy generation within a circular cross section tube subjected to

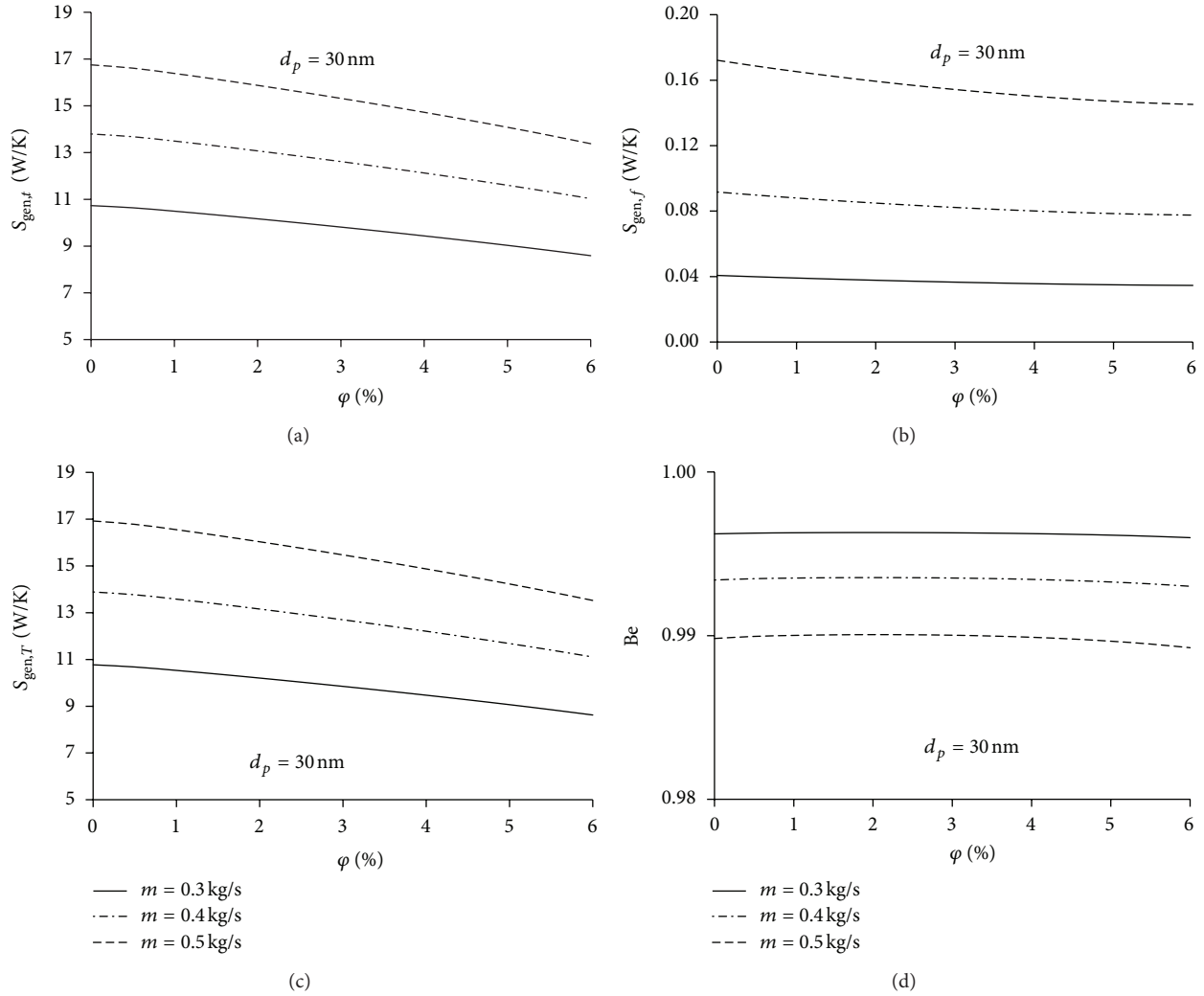


FIGURE 5: Entropy generation for constant mass flow rate inlet condition and for $d_p = 30$ nm: (a) thermal entropy generation; (b) frictional entropy generation; (c) total entropy generation; (d) Bejan number.

constant wall temperature and different inlet conditions. The tube has a length, L , equal to 1 m and a diameter, D , of 1 cm, Figure 1(a), whereas the temperature at the inlet, T_0 , is equal to 293 K and the temperature on the wall is 350 K.

Different inlet conditions are considered, namely, fixed Reynolds number, Re , in the range of $20 \cdot 10^3$ up to $100 \cdot 10^3$, constant mass flow rate from 0.3 up to 0.5 kg/s, and fixed inlet velocity ranging from 4.0 up to 8.5 m/s. All the above mentioned inlet conditions cause a turbulent flow with Re in the range of $11 \cdot 10^3$ until $100 \cdot 10^3$.

2.2. Thermophysical Properties. Definition of thermophysical properties of a nanofluid is extremely important, in order to determine reliable results, and different models to describe their behavior are available in the literature, as discussed in [31].

Density of nanofluids is calculated according to the general formula for the mixtures, obtaining the following

relation

$$\rho_{nf} = (1 - \phi) \rho_{bf} + \phi \rho_p \tag{1}$$

Specific heat is calculated by assuming thermal equilibrium between the nanoparticles and the base fluid by means of the following equation:

$$C_{p,nf} = \frac{(1 - \phi) \rho_{bf} C_{p,bf} + \phi \rho_p C_{p,p}}{\rho_{nf}} \tag{2}$$

As reported in [1], (1) and (2) have been validated experimentally, and they meet the general agreement of the scientific community.

Viscosity and thermal conductivity are calculated according to the correlations proposed by Corcione [2, 3]. These correlations are established by analyzing a large amount of experimental data available in the literature. According to [2],

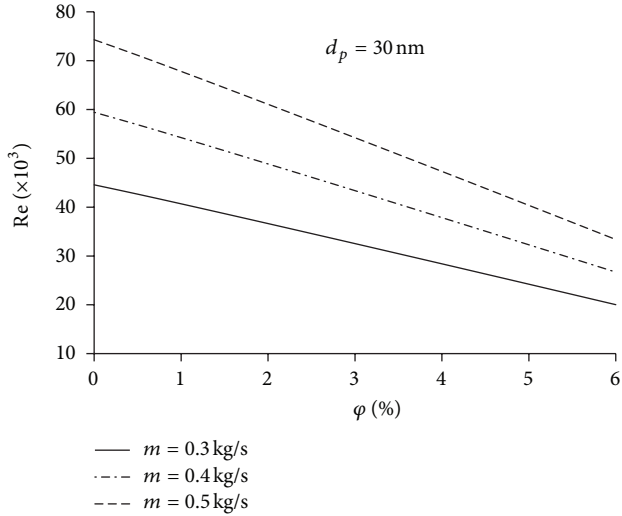


FIGURE 6: Reynolds number resulting from the constant mass flow rate inlet condition, in the case of $d_p = 30$ nm.

thermal conductivity of nanoparticles of spherical size can be expressed in the following way:

$$\frac{k_{nf}}{k_{bf}} = 1 + 4.4 \cdot \text{Re}_d^{0.4} \cdot \text{Pr}^{0.66} \cdot \left(\frac{T}{T_{fr}}\right)^{10} \cdot \left(\frac{k_p}{k_{bf}}\right)^{0.03} \cdot \varphi^{0.66}, \quad (3)$$

where Re_d is the nanoparticle Reynolds number and Pr is the Prandtl number of the base liquid. In more detail, the nanoparticle Reynolds number is defined as [2] follows:

$$\text{Re}_d = \frac{\rho_{bf} \cdot v_b \cdot d_p}{\mu_{bf}}, \quad (4)$$

where v_b is the Brownian velocity, defined as

$$v_b = \frac{2 \cdot C_B \cdot T}{\pi \cdot \mu_{bf} \cdot d_p^2}. \quad (5)$$

It can be noticed that (3) is a function of both nanoparticle concentration and diameter.

According to [3], dynamic viscosity can be expressed as

$$\frac{\mu_{nf}}{\mu_{bf}} = \frac{1}{1 - 24.3745 \cdot d_p^{-0.264} \cdot \varphi^{1.028}}. \quad (6)$$

Also, nanofluid dynamic viscosity is expressed as a function of particles diameter and concentration.

2.3. Mathematical Modeling. Figure 1 reports the configuration under investigation, Figure 1(a) particularly shows a schematic of all the considered domain, whereas in Figure 1(b), a sketch of a control volume used to develop the analysis is shown. The surface temperature of the duct is kept constant at T_w . An incompressible viscous fluid with mass flow rate equal to m and inlet temperature T_o enters the duct of length L and diameter D . Density, thermal conductivity,

and specific heat of the fluid are assumed to be constant within the range of temperatures considered in this study.

With reference to the control volume reported in Figure 1(b), an entropy balance can be written as

$$dS_{gen} = m \cdot ds - \frac{\delta Q}{T_w}. \quad (7)$$

And as reported in [32], for an incompressible fluid, ds can be expressed as follows:

$$ds = \frac{c_p \cdot dT}{T} - \frac{dp}{\rho \cdot T}, \quad (8)$$

whereas δQ is expressed as

$$\delta Q = m \cdot c_p \cdot dT. \quad (9)$$

Therefore, by substituting (8) and (9) into (7), the following expression is obtained:

$$dS_{gen} = m \cdot c_p \cdot \left(\frac{T_w - T}{T_w \cdot T} dT\right) - m \cdot \frac{dp}{\rho \cdot T}. \quad (10)$$

In (10), it is possible to distinguish different contributions. The first member of the equation represents the total entropy generation, whereas at the second member of the equation there are two terms: the first one is the thermal entropy generation, whereas the second one is the frictional entropy generation. Therefore, it is possible to write the following expression:

$$S_{gen,T} = S_{gen,t} + S_{gen,f}. \quad (11a)$$

Accordingly, Bejan number can be defined as

$$\text{Be} = \frac{S_{gen,t}}{S_{gen,T}} = \frac{S_{gen,t}}{S_{gen,t} + S_{gen,f}}. \quad (11b)$$

Be ranges from 0, all frictional irreversibility, to 1, all thermal irreversibility.

According to [32], from the integration of the first part of the second member of (10) between zero and the length of the duct, L , and by making some substitutions, the thermal entropy generation can be determined as follows:

$$S_{gen,t} = m \cdot c_p \cdot \left\{ \ln \left[\frac{1 - \tau \cdot e^{-4St\lambda}}{1 - \tau} \right] - \tau \cdot (1 - e^{-4St\lambda}) \right\}, \quad (12)$$

where τ is the dimensionless temperature, defined as

$$\tau = \frac{T_w - T_o}{T_w}, \quad (13)$$

and λ is the dimensionless length of the tube, defined as

$$\lambda = \frac{L}{D}, \quad (14)$$

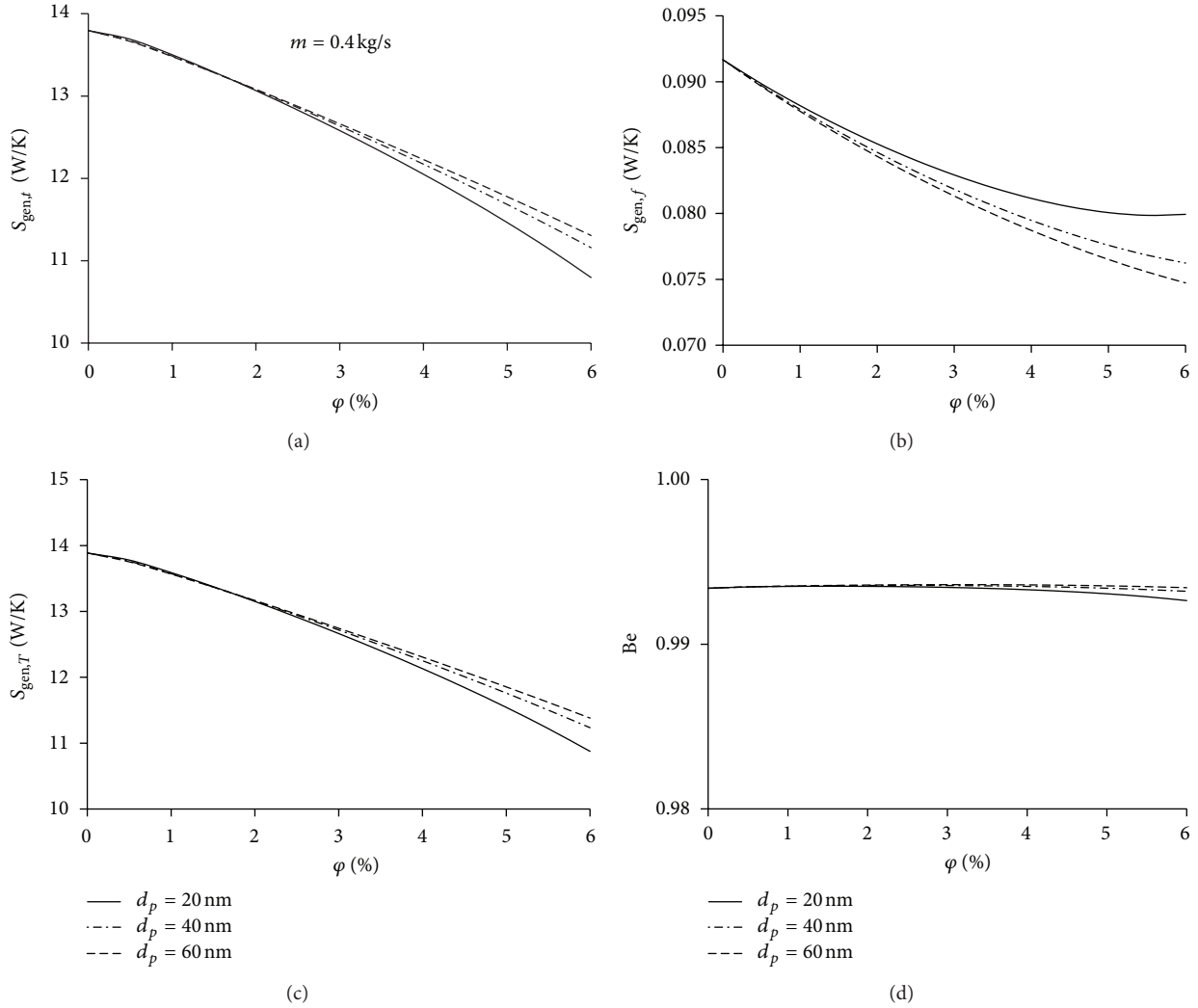


FIGURE 7: Entropy generation for constant mass flow rate inlet condition ($m = 0.4 \text{ kg/s}$) and different particles dimensions: (a) thermal entropy generation; (b) frictional entropy generation; (c) total entropy generation; (d) Bejan number.

and St is the Stanton number, expressed as

$$St = \frac{h}{\rho \cdot w \cdot c_p} = \frac{Nu}{Re Pr} \quad \text{with } Nu = \frac{hD}{k}, \quad (15)$$

and h representing the convection heat transfer coefficient, calculated from the correlation suggested by Pak and Cho, specifically developed for nanofluids [33]:

$$Nu = 0.021 \cdot Re^{0.8} \cdot Pr^{0.5}. \quad (16)$$

The frictional entropy generation can be expressed according to Bejan [34], by integrating the second part of the second member of (10):

$$S_{gen,f} = \frac{32 \cdot m^3 \cdot f \cdot L}{\rho^2 \cdot T_{ave} \cdot \pi^2 \cdot D^5}, \quad (17)$$

where f is the friction factor calculated as suggested in [25, 35], estimated as:

$$f = [0.79 \cdot \ln(Re) - 1.64]^{-2}, \quad (18)$$

and T_{ave} is the average bulk temperature of the fluid inside the tube, estimated as

$$T_{ave} = \frac{T_0 - T_{out}}{\ln(T_0/T_{out})}, \quad (19)$$

where T_{out} is determined as

$$T_{out} = T_w - (T_w - T_0) \cdot \exp\left(\frac{-h \cdot p \cdot L}{m \cdot c_p}\right). \quad (20)$$

3. Results and Discussion

Results are reported in terms of thermal, frictional, and total entropy generation and Bejan number, in order to understand the relative importance of thermal entropy generation with respect to frictional entropy generation.

For assigned d_p and ϕ , the terms $C_{p,nf}$, k_{nf} , and μ_{nf} are evaluated by (2), (3), and (6), respectively, and, consequently, the Pr value is obtained. Re allows the evaluation of Nu and St

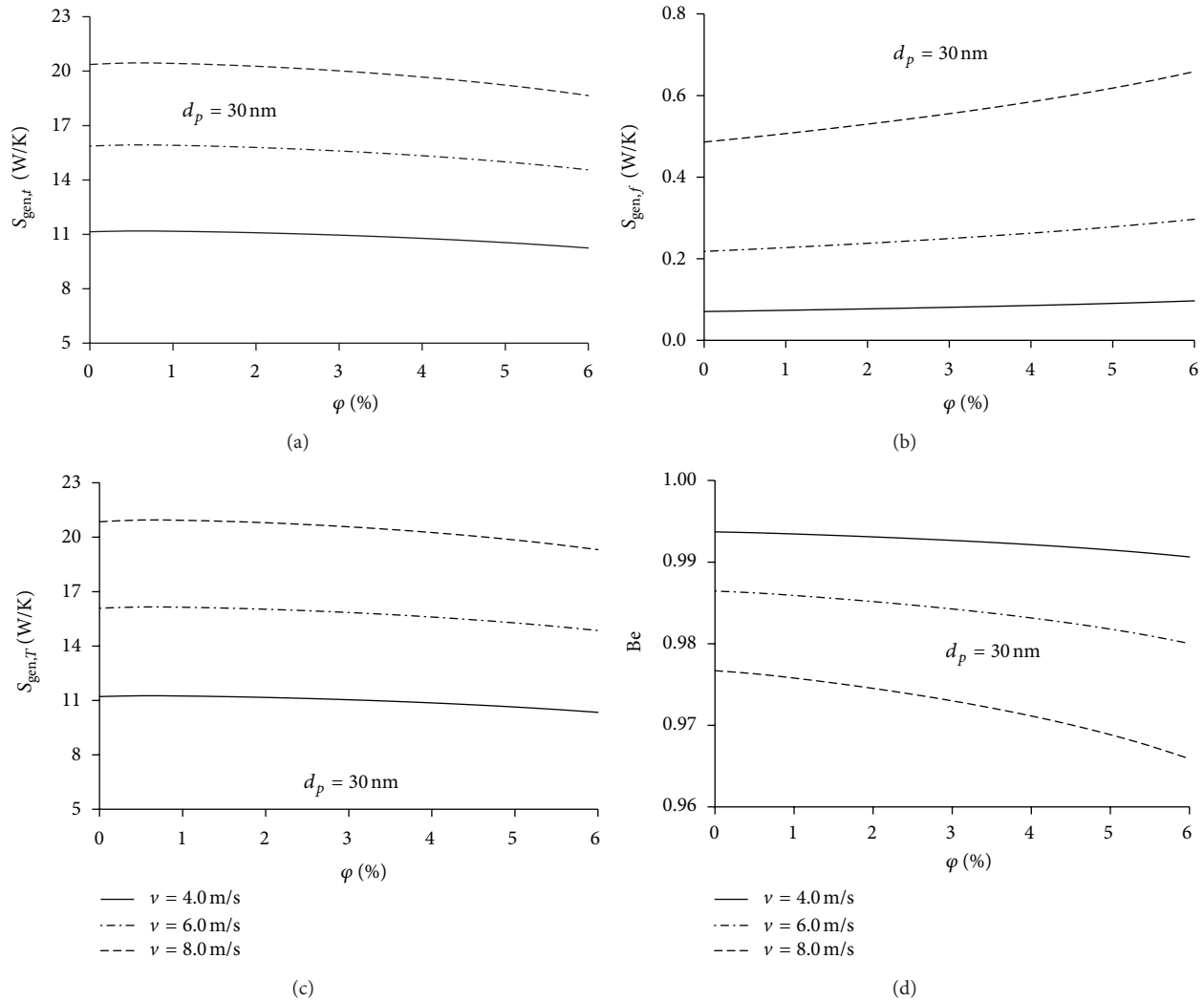


FIGURE 8: Entropy generation for constant velocity inlet condition and for $d_p = 30$ nm: (a) thermal entropy generation; (b) frictional entropy generation; (c) total entropy generation; (d) Bejan number.

values by (16) and f by (18). Thermal and frictional entropy generations are evaluated by (12) and (17) for assigned τ , equal to 0.163 (i.e., in the present study τ is kept constant).

First of all, the impact of possible deviations affecting the correlation of Nu (16) on the thermal entropy generation is analyzed. It is considered a variation of Nu of $\pm 20\%$ with respect to the value calculated by (16). The case of constant $Re = 60 \cdot 10^3$, particles diameter equal to 30 nm, and variable volumetric concentration is taken into account.

Figure 2 reveals that for a variation of Nu of $+20\%$, there is an increase of thermal entropy generation between 12% and 13%; therefore, the effect of a positive deviation in Nu is smoothed. When there is a variation in Nu of -20% , there is a decrease of thermal entropy generation varying between -14% and -15% ; therefore, a smoothing effect is still present.

Figure 2 shows that when possible experimental deviations of Nu are taken into account, there is a variation in the value of thermal entropy generation, but the trend is similar; therefore, the main considerations (i.e., optimal

concentration of nanoparticles) are not affected by possible experimental deviation of (16).

Figure 3 shows the analysis for constant Re as inlet condition and for a fixed particles dimension ($d_p = 30$ nm), whereas the volumetric concentration varies.

In Figure 3, it is detected an increase of thermal, frictional, and total entropy generation at the increase of concentration, whereas Be number decreases highlighting that as concentration increases the frictional entropy generation starts to give a substantial contribution to the total irreversibility of the system.

The reported behavior can be explained in the following way: at the increase of the concentration there is a growth of both density and dynamic viscosity, but the increase of the latter contribution is much stronger; therefore, in order to maintain Re constant, it is necessary to increase the velocity, which, in turn, determines a strong increase of the mass flow rate. The increase of the mass flow rate is higher than the decrease of the specific heat (see (12)), whereas the effect of

the other terms in (12) is limited; therefore, thermal entropy generation grows.

In the same way, also the frictional entropy generation increases (see (17)), but as a cubic function of the mass flow rate; that way at higher concentration, it starts to affect the total entropy generation.

Figure 4 reports the aforementioned analysis for constant Re ($Re = 50 \cdot 10^3$) and different dimensions of the particles (20 nm, 40 nm, and 60 nm), showing that as the diameters decrease, entropy generation increases, whereas Be number reduces.

This behavior is due to the fact that as particles dimensions decrease, there is a strong increase of the dynamic viscosity (see (6)), caused by the higher surface of interaction among the particles and base fluid (at constant concentration, smaller particles have a higher total surface of interaction with the base fluid). If the viscosity grows, it is necessary a higher velocity to have a constant Re, as previously mentioned.

Figure 5 illustrates the results when mass flow rate is kept constant assuming three different conditions (0.3 kg/s, 0.4 kg/s, and 0.5 kg/s) and particles dimension is taken fixed ($d_p = 30$ nm), whereas particles concentration is variable. It can be noticed that thermal, frictional, and total entropy generations tend to reduce, whereas Be number is nearly constant, showing a proportional variation of thermal and frictional generation; even though it is to be noticed that thermal entropy generation is much higher than frictional entropy generation.

This behavior is due to the fact that, by keeping mass flow rate constant and increasing the concentration of the nanoparticles, there is a decrease of the specific heat, which determines most of the reduction of thermal entropy generation, and an increase of the density, which causes most of the decrease of the frictional entropy generation. These two contributions have a similar effect, therefore Be number remains nearly constant. Anyway, as previously noticed, the impact of specific heat is more relevant, because thermal entropy generation is two order of magnitude higher with respect to thermal entropy generation.

Moreover it is important to consider that by keeping mass flow rate constant, a significant reduction of Re is determined (Figure 6) as concentration increases. This, according to (16), determines a reduction of Nu; therefore, when mass flow rate is kept constant there is a more efficient (i.e., entropy generation decreases) but less effective heat exchange (i.e., a lower quantity of heat is exchanged).

Figure 7 reports entropy generation and Be number for a constant mass flow rate (0.4 kg/s), three different nanoparticles dimensions (20 nm, 40 nm, and 60 nm), and variable concentration.

From Figure 7, it is noticed an opposite trend of thermal and frictional entropy generation; in fact, thermal entropy generation tends to decrease with the nanoparticles diameters, whereas the opposite happens for frictional generation. The overall effect is a decrease of the total entropy generation, when particles dimensions reduce, because the weight of thermal entropy generation is much higher with respect to frictional thermal generation.

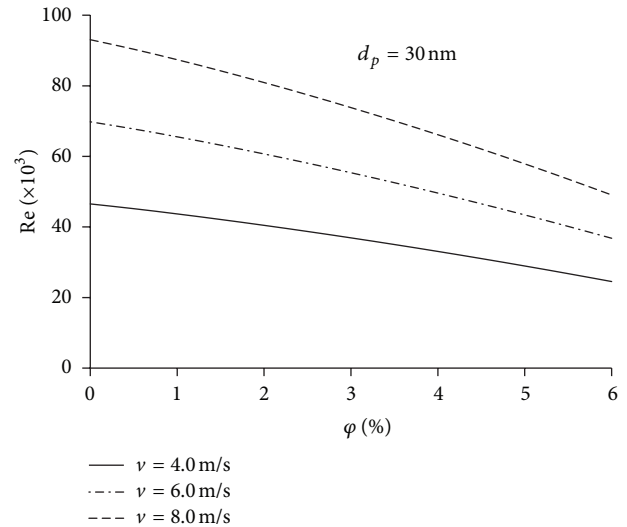


FIGURE 9: Reynolds number resulting from the constant velocity inlet condition, in the case of $d_p = 30$ nm.

Thermal entropy generation decreases, because the reduction of the particles dimensions causes a reduction of the Stanton number, which makes thermal entropy generation decrease according to (12).

The reduction of St is due to a decrease of Nu caused by the reduction of Re due to the increase of dynamic viscosity determined by the decrease of particles dimensions (i.e., the decrease of the amount of heat transferred to the nanofluid is stronger than the decrease of the nanofluid heat capacity, provoking a reduction of St).

The same mechanism is also responsible for the increase of frictional entropy generation; in fact, as Re decreases, f increases (18), provoking a rise of the frictional entropy generation (17).

Figure 8 reports the results for the case of constant inlet velocity, taking into account three different values (4 m/s, 6 m/s, and 8 m/s), a particles dimension equal to 30 nm, and concentration between 0% and 6%.

It is detected a decrease of the thermal entropy generation and an increase of frictional entropy generation. The overall effect is a slight decrease of total entropy generation, because frictional entropy generation is one order of magnitude lower than thermal entropy generation, thus, Be number has a value close to 1.

Thermal entropy generation decreases as concentration increases (except for low concentration, as shown and discussed in the following), because at the increase of concentration there is a reduction of the specific heat, which is stronger than the effect of the increase of the mass flow rate, caused by the rise of the density. Moreover, St number decreases, contributing to the reduction of thermal entropy generation for the previously mentioned reasons. The reduction of St is due to the decrease of Nu provoked by the decrease of Re at the increase of particles concentration (Figure 9). Re decreases because the rise of viscosity is more significant than that of density.

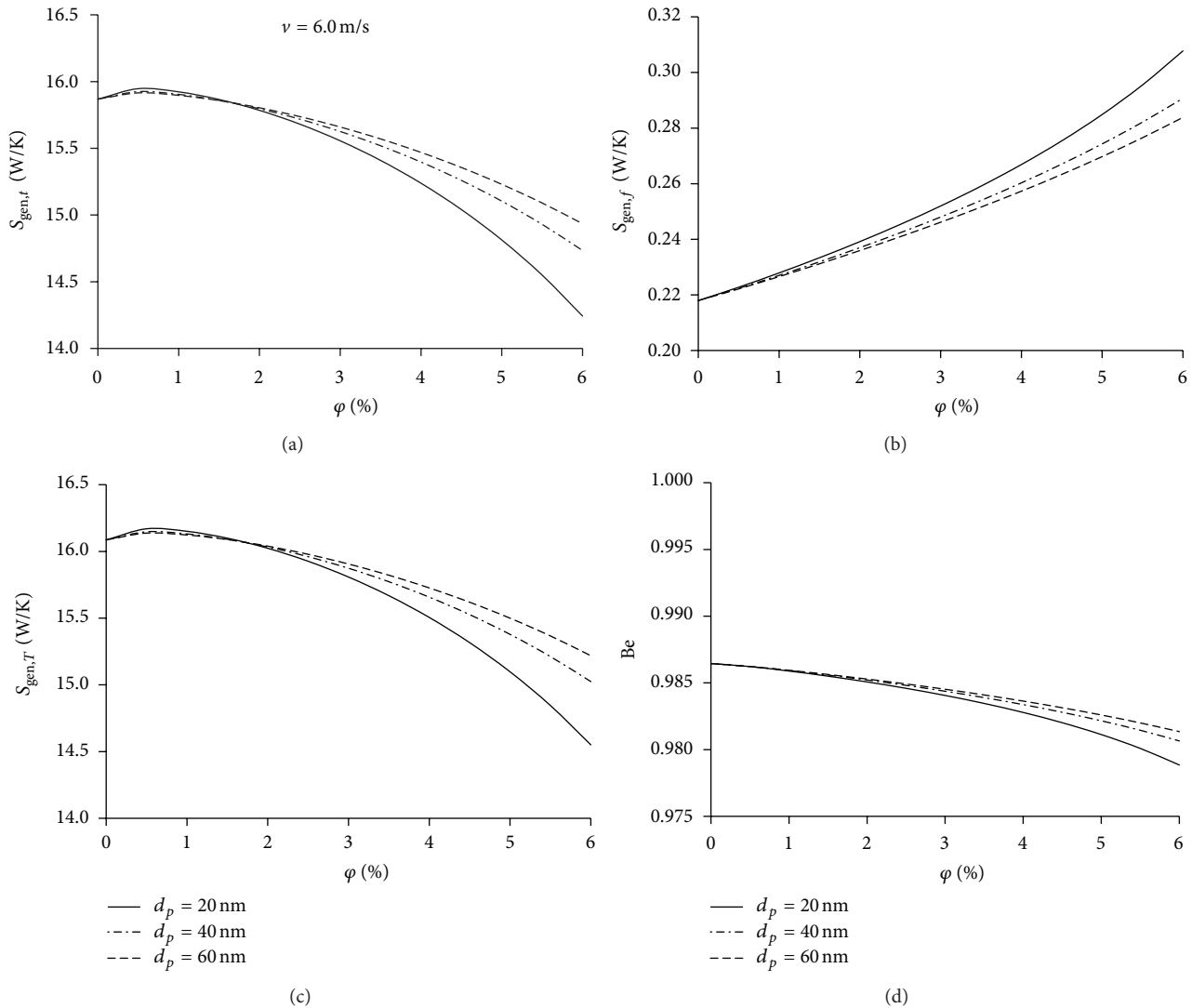


FIGURE 10: Entropy generation for constant velocity inlet condition ($v = 6.0$ m/s) and different particles dimensions: (a) thermal entropy generation; (b) frictional entropy generation; (c) total entropy generation; (d) Bejan number.

On the contrary, frictional entropy generation increases, because the effect of the increase of the mass flow rate and of the frictional coefficient are dominant, with respect to other mechanisms which tend to reduce frictional entropy generation (i.e., increase of density).

Figure 10 shows the trend of thermal, frictional, and total entropy generation, together with Be , for a value of velocity of 6.0 m/s and different particles dimensions (20 nm, 40 nm, and 60 nm) as a function of the concentration. It is detected that, as previously mentioned, there is a substantial decrease of thermal entropy generation, except for concentration up to 1% . The increase of entropy generation is due to the increase of St , caused by the increase of heat convection coefficient driven by the rise of thermal conductivity. At low concentration, this effect and the increase of mass flow rate are dominant with respect to the decrease of the specific heat. As concentration increases (i.e., after 1%), the reduction of Re , determined by the increase of the viscosity, causes a strong

reduction of Nu , and the increase of the thermal conductivity is not sufficient to make St increase, so it starts to decrease, contributing to the reduction of thermal entropy generation.

The reduction of thermal entropy generation caused by the reduction of particles dimensions is due to reasons analogous to what happened in the case of mass flow rate (i.e., reduction of St at the decrease of particles dimensions), the same is for the increase of frictional entropy generation (decrease of Re with consequent increase of f).

4. Conclusions

The present paper investigated the entropy generation of a nanofluid turbulent convection flow within a circular cross section tube subjected to constant wall temperature. The analysis showed that the considered inlet condition influences the different mechanisms and the amount of entropy generation. Particularly, it is shown that at constant Re there is an increase

of both thermal and frictional entropy generation, with a higher increase of frictional entropy generation according to the rise of particles concentration.

For constant mass flow rate and inlet velocity, more similar trends are observed. Specifically, there is a decrease of thermal entropy generation for both cases, whereas frictional entropy generation decreases in the case of constant mass flow rate and increases for constant velocity inlet condition. For these two conditions, an overall decrease of the total entropy generation is detected.

It is very important to highlight that a dominant role in the analysis of the considered problem is played by dynamic viscosity, which has a strong influence on the resulting Re, when it is not assumed constant.

Nomenclature

A:	Area (m^2)
Be:	Bejan number
C_B :	Boltzmann's constant = $1.38066 \times 10^{-23} \text{ J K}^{-1}$
C_p :	Specific heat ($\text{kJ kg}^{-1} \text{ K}^{-1}$)
D:	Tube diameter (m)
d_p :	Particle diameter (nm)
f:	Friction factor
h:	Convective heat transfer coefficient ($\text{W m}^{-2} \text{ K}^{-1}$)
k:	Thermal conductivity ($\text{W m}^{-1} \text{ K}^{-1}$)
L:	Tube length (m)
Nu:	Nusselt number
m:	Mass flow rate (kg s^{-1})
p:	Pressure (Pa)
P:	Perimeter (m)
Pr:	Prandtl number, $\mu C_p/k$
q:	Heat flux (W m^{-2})
q' :	Heat transfer per unit of length (W m^{-1})
Re:	Reynolds number
S_{gen} :	Entropy generation (W K^{-1})
S'_{gen} :	Entropy generation per unit of length ($\text{W K}^{-1} \text{ m}^{-1}$)
St:	Stanton number
T:	Temperature (K)
x:	Axial coordinate (m)
v:	Velocity (m s^{-1}).

Greek Symbols

φ :	Particles concentration
μ :	Dynamic viscosity (N s m^{-2})
ρ :	Density (kg m^{-3}).

Subscripts

Ave:	Average
b:	Brownian
bf:	Base fluid
d:	Nanoparticle diameter
f:	Frictional
fr:	Freezing.

g:	Generation
h:	Hydraulic
in:	Inlet
nf:	Nanofluids
out:	Outlet
p:	Particles
t:	Thermal
T:	Total.

References

- [1] K. Khanafer and K. Vafai, "A critical synthesis of thermophysical characteristics of nanofluids," *International Journal of Heat and Mass Transfer*, vol. 54, no. 19-20, pp. 4410–4428, 2011.
- [2] M. Corcione, "Empirical correlating equations for predicting the effective thermal conductivity and dynamic viscosity of nanofluids," *Energy Conversion and Management*, vol. 52, no. 1, pp. 789–793, 2011.
- [3] M. Corcione, "A semi-empirical model for predicting the effective dynamic viscosity of nanoparticle suspensions," *Heat Transfer Engineering*, vol. 33, no. 7, pp. 575–583, 2012.
- [4] J. Fan and L. Wang, "Review of heat conduction in nanofluids," *Journal of Heat Transfer*, vol. 133, no. 4, Article ID 040801, 2011.
- [5] J. Buongiorno, "Convective transport in nanofluids," *Journal of Heat Transfer*, vol. 128, no. 3, pp. 240–250, 2006.
- [6] K. Khanafer, K. Vafai, and M. Lightstone, "Buoyancy-driven heat transfer enhancement in a two-dimensional enclosure utilizing nanofluids," *International Journal of Heat and Mass Transfer*, vol. 46, no. 19, pp. 3639–3653, 2003.
- [7] V. Bianco, F. Chiacchio, O. Manca, and S. Nardini, "Numerical investigation of nanofluids forced convection in circular tubes," *Applied Thermal Engineering*, vol. 29, no. 17-18, pp. 3632–3642, 2009.
- [8] Y. He, Y. Men, Y. Zhao, H. Lu, and Y. Ding, "Numerical investigation into the convective heat transfer of TiO_2 nanofluids flowing through a straight tube under the laminar flow conditions," *Applied Thermal Engineering*, vol. 29, no. 10, pp. 1965–1972, 2009.
- [9] S. Tahir and M. Mital, "Numerical investigation of laminar nanofluid developing flow and heat transfer in a circular channel," *Applied Thermal Engineering*, vol. 39, pp. 8–14, 2012.
- [10] A. Behzadmehr, M. Saffar-Avval, and N. Galanis, "Prediction of turbulent forced convection of a nanofluid in a tube with uniform heat flux using a two phase approach," *International Journal of Heat and Fluid Flow*, vol. 28, no. 2, pp. 211–219, 2007.
- [11] S. Mirmasoumi and A. Behzadmehr, "Numerical study of laminar mixed convection of a nanofluid in a horizontal tube using two-phase mixture model," *Applied Thermal Engineering*, vol. 28, no. 7, pp. 717–727, 2008.
- [12] V. Bianco, O. Manca, and S. Nardini, "Numerical investigation on nanofluids turbulent convection heat transfer inside a circular tube," *International Journal of Thermal Sciences*, vol. 50, no. 3, pp. 341–349, 2011.
- [13] V. Bianco, O. Manca, and S. Nardini, "Numerical simulation of water/ Al_2O_3 nanofluid turbulent convection," *Advances in Mechanical Engineering*, vol. 2010, Article ID 976254, 10 pages, 2010.
- [14] M. Hejazian and M. K. Moraveji, "A comparative analysis of single and two-phase models of turbulent convective heat transfer in a tube for TiO_2 nanofluid with CFD," *Numerical Heat Transfer A*, vol. 63, no. 10, pp. 795–806, 2013.

- [15] K. M. Moraveji and E. Esmaeili, "Comparison between single-phase and two-phases CFD modeling of laminar forced convection flow of nanofluids in a circular tube under constant heat flux," *International Communications in Heat and Mass Transfer*, vol. 39, no. 8, pp. 1297–1302, 2012.
- [16] K. V. Wong and O. de Leon, "Applications of nanofluids: current and future," *Advances in Mechanical Engineering*, vol. 2010, Article ID 519659, 11 pages, 2010.
- [17] M. Shafahi, V. Bianco, K. Vafai, and O. Manca, "An investigation of the thermal performance of cylindrical heat pipes using nanofluids," *International Journal of Heat and Mass Transfer*, vol. 53, no. 1–3, pp. 376–383, 2010.
- [18] M. Shafahi, V. Bianco, K. Vafai, and O. Manca, "Thermal performance of flat-shaped heat pipes using nanofluids," *International Journal of Heat and Mass Transfer*, vol. 53, no. 7–8, pp. 1438–1445, 2010.
- [19] K. Alizad, K. Vafai, and M. Shafahi, "Thermal performance and operational attributes of the startup characteristics of flat-shaped heat pipes using nanofluids," *International Journal of Heat and Mass Transfer*, vol. 55, no. 1–3, pp. 140–155, 2012.
- [20] O. Manca, S. Nardini, and D. Ricci, "A numerical study of nanofluid forced convection in ribbed channels," *Applied Thermal Engineering*, vol. 37, pp. 280–292, 2012.
- [21] R. Krishna Sabareesh, N. Gobinath, V. Sajith, S. Das, and C. B. Sobhan, "Application of TiO₂ nanoparticles as a lubricant-additive for vapor compression refrigeration systems—an experimental investigation," *International Journal of Refrigeration*, vol. 35, no. 7, pp. 1989–1996, 2012.
- [22] O. Mahian, A. Kianifar, S. A. Kalogirou, I. Pop, and S. Wongwises, "A review of the applications of nanofluids in solar energy," *International Journal of Heat and Mass Transfer*, vol. 57, no. 2, pp. 582–594, 2013.
- [23] O. Mahian, S. Mahmud, and S. Zeinali Heris, "Effect of uncertainties in physical properties on entropy generation between two rotating cylinders with nanofluids," *Journal of Heat Transfer*, vol. 134, no. 10, Article ID 101704, 2012.
- [24] O. Mahian, S. Mahmud, and S. Z. Heris, "Analysis of entropy generation between co-rotating cylinders using nanofluids," *Energy*, vol. 44, no. 1, pp. 438–446, 2012.
- [25] K. Y. Leong, R. Saidur, T. M. I. Mahlia, and Y. H. Yau, "Entropy generation analysis of nanofluid flow in a circular tube subjected to constant wall temperature," *International Communications in Heat and Mass Transfer*, vol. 39, no. 8, pp. 1169–1175, 2012.
- [26] K. Y. Leong, R. Saidur, M. Khairulmaini, Z. Michael, and A. Kamyar, "Heat transfer and entropy analysis of three different types of heat exchangers operated with nanofluids," *International Communications in Heat and Mass Transfer*, vol. 39, no. 6, pp. 838–843, 2012.
- [27] M. Moghaddami, A. Mohammadzade, and S. A. V. Esfehiani, "Second law analysis of nanofluid flow," *Energy Conversion and Management*, vol. 52, no. 2, pp. 1397–1405, 2011.
- [28] P. K. Singh, K. B. Anoop, T. Sundararajan, and S. K. Das, "Entropy generation due to flow and heat transfer in nanofluids," *International Journal of Heat and Mass Transfer*, vol. 53, no. 21–22, pp. 4757–4767, 2010.
- [29] V. Bianco, S. Nardini, and O. Manca, "Enhancement of heat transfer and entropy generation analysis of nanofluids turbulent convection flow in square section tubes," *Nanoscale Research Letters*, vol. 6, no. 1, article 252, 2011.
- [30] V. Bianco, O. Manca, and S. Nardini, "Entropy generation analysis of turbulent convection flow of Al₂O₃-water nanofluid in a circular tube subjected to constant wall heat flux," *Energy Conversion and Management*, vol. 77, pp. 306–314, 2014.
- [31] V. Bianco, S. Nardini, and O. Manca, "Heat transfer in nanofluids," in *Advances in Industrial Heat Transfer*, A. A. Minea, Ed., pp. 165–200, CRC Press, New York, NY, USA, 2013.
- [32] A. Z. Şahin, "Entropy generation in turbulent liquid flow through a smooth duct subjected to constant wall temperature," *International Journal of Heat and Mass Transfer*, vol. 43, no. 8, pp. 1469–1478, 2000.
- [33] B. C. Pak and Y. I. Cho, "Hydrodynamic and heat transfer study of dispersed fluids with submicron metallic oxide particles," *Experimental Heat Transfer*, vol. 11, no. 2, pp. 151–170, 1998.
- [34] A. Bejan, *Entropy Generation Minimization*, CRC Press, Boca Raton, Fla, USA, 1996.
- [35] F. P. Incropera and D. P. DeWitt, *Fundamentals of Heat Transfer*, John Wiley & Sons, New York, NY, USA, 1995.